Kinematic Behavior of Geogrid Reinforcements during Earthquakes

Ahmed Hosny Abdel-Rahman, Mohamed Abdel-Moneim

Abstract—Reinforced earth structures are generally subjected to cyclic loading generated from earthquakes. This paper presents a summary of the results and analyses of a testing program carried out in a large-scale multi-function geosynthetic testing apparatus that accommodates soil samples up to 1.0 m^3. This apparatus performs different shear and pullout tests under both static and cyclic loading. The testing program was carried out to investigate the controlling factors affecting soil/geogrid interaction under cyclic loading. The extensibility of the geogrids, the applied normal stresses, the characteristics of the cyclic loading (frequency, and amplitude), and initial static load within the geogrid sheet were considered in the testing program. Based on the findings of the testing program, the effect of these parameters on the pullout resistance of geogrids, as well as the displacement mobility under cyclic loading were evaluated. Conclusions and recommendations for the design of reinforced earth walls under cyclic loading are presented.

Keywords—Geogrid, Soil, Interface, Cyclic Loading, Pullout, and Large scale Testing.

I. INTRODUCTION

GEOTECHNICAL performance of soil/reinforcement interaction subjected to monotonic pullout loading has been well investigated in the literature [3], [12], [9]. However, the same interaction under the effect of cyclic pullout loading still need to be further investigated [5]. However, it is recently recognized that further in-depth investigations are required to define the effect of the controlling factors on this interaction and incorporate them within the design schemes of reinforced earth structures [6].

Within the last two decades, only a few reinforced earth structures were reported in the literature to have experienced failure during earthquakes. Fig. 1 shows a view for collapsed reinforced earth walls during earthquakes in the USA (Fig. 1 (a)) and Taiwan (Fig. 1 (b)). The majority of the earth retaining structures showed good performance at the time when the rest of the surrounding structures have failed [7], [4], [5], [10], [8], and [11]. Researchers have related these failures to insufficient pullout resistance, increase in the slippage displacement of the geogrids within the anchorage zone, connection failure between the geogrid sheets and the facing, or inadequacy of the safety factors against global stabilities. The different modes of failure of a reinforced earth structure under static and/or cyclic loading are presented in Fig. 2.

Ahmed Hosny Abdel-Rahman, Professor, is with the National Research Center, Cairo, Egypt (phone: +201001423357; fax: +202-22757417; e-mail: ahosny66@hotmail.com).

Mohamed Abdel-Moneim, Assistant Professor, is with the National Research Center, Cairo (e-mail: abdmoniem2000@yahoo.com).

This paper presents a study on the behavior of soil/geogrid interaction along the anchorage zone under cyclic pullout loading. The study was based on a comprehensive laboratory cyclic pullout tests. A series of static and cyclic pullout tests were carried out throughout the course of this research to investigate the different controlling parameters that affect the pullout strength and displacement mobility of geogrid sheets subjected to cyclic loading. The tests were carried out using a large scale testing apparatus of an internal dimension of nearly 1.0 m^3.

Fig. 1 Collapsed Reinforced Earth Walls During Earthquakes. (a) Extended Stay Hotel MSE Wall-Seattle collapsed after the Nisqually earthquake (USA-PEER 2001), (b) Collapsed Wall at Highway 129 after Chi Chi Earthquake [5]

II. TESTING APPARATUS

The following sections describe the pullout testing apparatus, the basic properties of the materials used in the testing program, the testing procedure, as well as the testing matrix.

A. Description of the Apparatus

Fig. 3 presents a photographic view of the testing apparatus. The testing apparatus was manufactured and designed at the

National Research Center of Egypt [1]. The apparatus is of internal dimensions 1.2 m x 0.8m x 1.00 m for length, width and height; respectively. It is capable of performing three types of tests (uniaxial tension tests on geogrids, direct shear tests on soils, and pullout tests of geogrids from soils) in both monotonic and cyclic loading conditions. The following sections describe the loading and instrumentation systems of the apparatus;
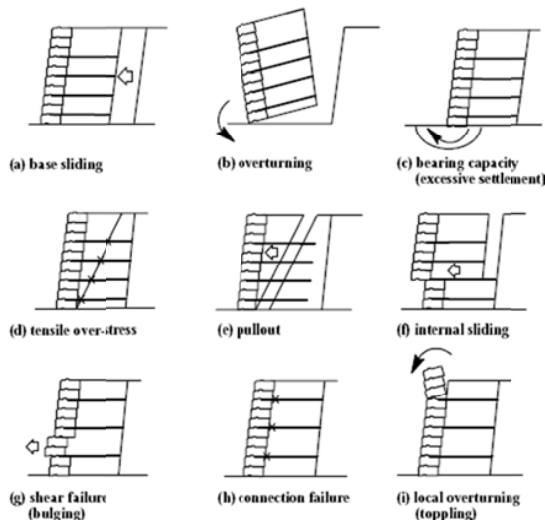

Fig. 2 Different Modes of Failure of Reinforced Earth Retaining Walls under Static and/or Seismic Conditions [2]

B. The Loading System

A vertical reaction frame is designed to resist 20 ton reaction forces from two vertical hydraulic jacks that simulate loads from in situ pressure. Another reaction frame is designed to resist a 25 ton horizontal force applied from a horizontal jack. That load could be used to pull a reinforcing sheet or to mobilize the lower box in a direct shear test. The horizontal loading system is operated through a load control system.

Fig. 3 General View of the Testing Apparatus

In order to simulate the cyclic horizontal loading, a proportional electric relief valve (capacity 200 bar) is attached to the horizontal jack as shown in Fig. 4. A control system is attached to this valve, and signals are transferred to the control system through a data acquisition card with corresponding NI-DAQ software and in-house coded software on a personal computer. The program can generate four types of waves (square, sinusoidal, saw tooth and ramp wave). A series of four subsequent waves could be generated. The maximum frequency of the new system is 3 Hz.

The program transmits the signal to the control unit and the control unit transmits the electric signal to the electric relief valve which applies the cyclic horizontal load.

C. The Instrumentation System

Fig. 4 presents elevation and planar views for the apparatus with its instrumentation system. The utilized instrumentation system consists of the following;

1. Dynamic data logger; includes two units of sensor interface model PCD 320, with a sampling frequency of up to 500 Hz. A junction terminal box, with its corresponding amplifier, acts as a transition between the different sensors and the data logger system.
2. A load cell of capacity 500 kN is placed between the horizontal hydraulic jack and reaction frame.
3. A pressure cell is located beneath the sheet level at the shearing level to measure the changes in the normal stresses around the shearing surface. This is in addition to a pressure sensors attached to the hydraulic pump, to measure the pressure of the vertical hydraulic jacks.
4. Four LVDTs of maximum measuring distance ranges between 100 to 150 mm connected along the geogrid sheet during pullout; at distances 5, 27, 49, and 71 cm, measured from the loaded front of the sheet.

III. MATERIALS

A. Utilized Soil

The tested soil was a medium to fine siliceous sand with "D50" of 0.60 mm as shown in Fig. 5. A static direct shear tests, performed on that sand using the large scale apparatus, showed that the peak value of angle of internal friction (Φ) is 33° at 1.75 t/m^3 dry density and 94 % relative compaction.

B. Geogrids

Five types of geogrids of different stiffnesses, A, B, C, D and E were used in the experimental testing program. All tested geogrids were mono-oriented of HDPE (Highly Density Polyethylene) type. The dimensional characteristics are summarized in Table I, while the mechanical characteristics are given in Table II. Fig. 6 shows the stress-strain curves of the different types of geogrids obtained from the manufacturer.

IV. TESTING PROCEDURE

The tested samples were monotonically loaded to a certain load (static pullout load level–referred to in this paper as

"Static Pullout Load Level - SPLL") then cyclic loading started, at a specified loading frequency and amplitude (minimum and maximum around the static pullout load level). Fig. 7 illustrates the cyclic loading technique.

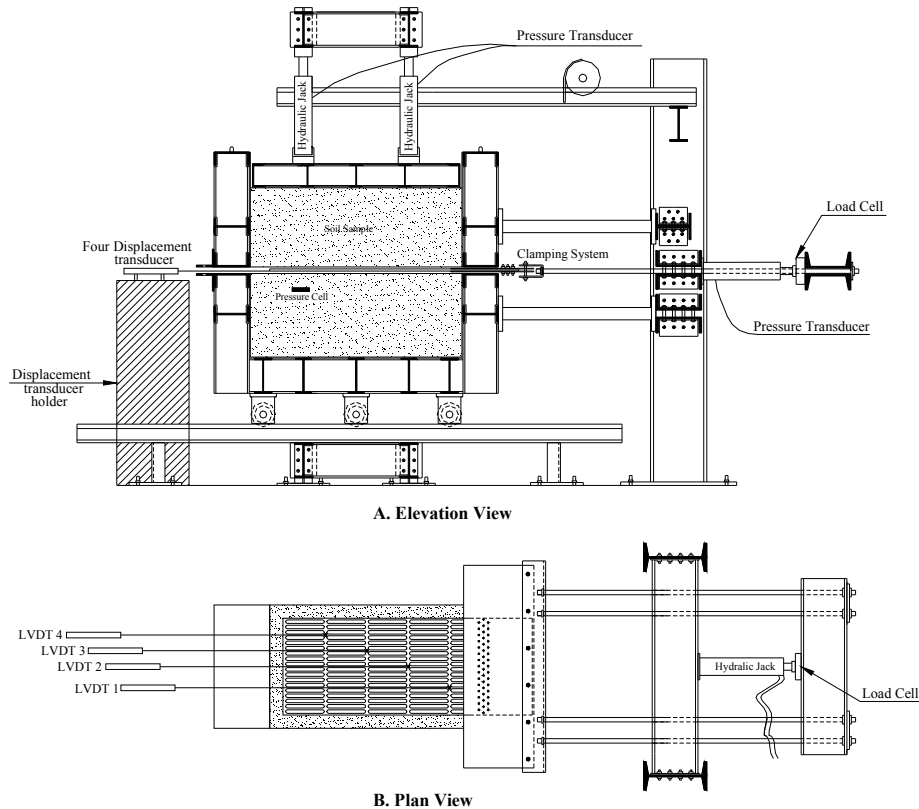**A. Elevation View**

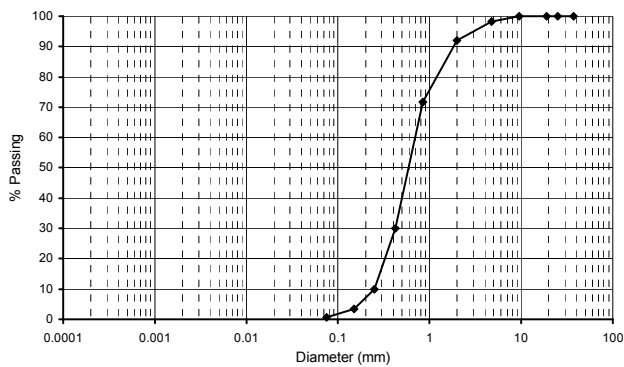**B. Plan View**

Fig. 4 Plan and Elevation Showing the Instrumentation Devices

Fig. 5 Grain Size Distribution of the Tested Sand

TABLE I
GEOMETRICAL PROPERTIES OF THE TESTED GEOGRIDS

Item	A	B	C	D	E
Aperture Size (M.D) (mm)	220	220	220	220	220
Aperture Size (T.D) (mm)	13/20	13/20	13/20	13/20	13/20
Mass per Unit Area (g/m²)	1000	800	600	400	300

M. D: Machine Direction; T.D.: Transverse Direction (Refer to Fig. 9)

V. TESTING MATRIX

For each geogrid type, a matrix of static and cyclic loading tests was carried out. The testing matrix was designed to cover the most important factors that control the behavior of geogrid sheets under cyclic pullout loads including stiffness of geogrid, interface normal stresses (σ_{ni}), initial Static Pullout Load Level (SPLL) within the geogrid, and frequency of loading (F_L).

TABLE II
MECHANICAL CHARACTERISTICS OF THE TESTED GEOGRIDS

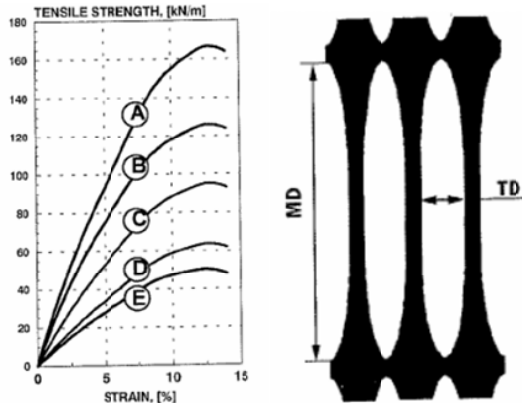| Item	A	B	C	D	E
Tensile Strength at 2% Strain (kN/m)	45	36	26	17	11
Tensile Strength at 5% Strain (kN/m)	90	72	50	32	25
Peak Tensile Strength (kN/m)	160	120	90	60	45
Yield Point Elongation (%)	13	13	13	13	11.5
Junction Strength (kN/m)	130	110	80	50	36
Long Term Design Strength (kN/m)	75.4	56.5	42.4	28.3	21.2

Fig. 6 Stress-Strain Relationships of the Tested Geogrid Types
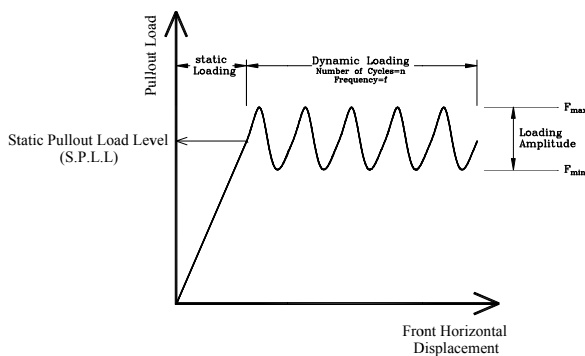

Fig. 7 Cyclic Loading Sequence Adopted in the Tests

VI. Tests Results

Figs. 8-11 show samples of the tests results for geogrids type A, B, and C only in both static and cyclic conditions under different loading and frequency conditions.
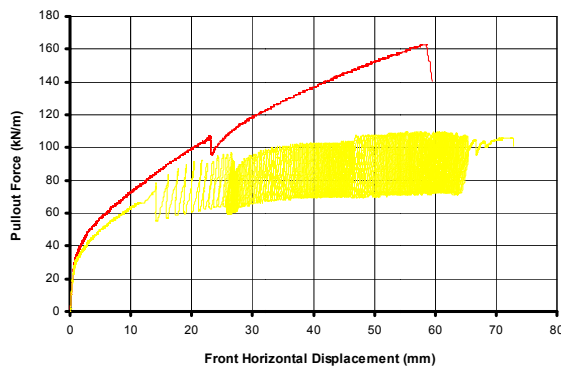

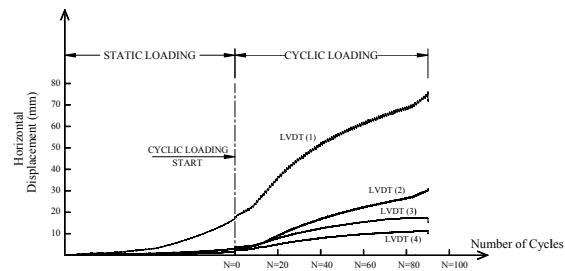Fig. 8 Static and Cyclic Pullout Tests Results of Geogrid A at (FL=1.0 Hz, σ_{ni} = 52 kPa, SPLL = 80 kPa)

Fig. 9 Horizontal Displacements of the LVDTs along Geogrid A (FL=1.0 Hz, σ_{ni} =52 kPa, SPLL=80 kPa)

VII. Factors Affecting Soil/Geogrid Interaction Under Cyclic Loading

Based on comparisons on the results of the experimental investigation, the following sections present the effect of different controlling factors on the behavior of soil/geogrid interface during static and cyclic pullout loading.

A. Effect of Geogrid Extensibility on the Pullout Response

The responses of Geogrids B and C during cyclic pullout tests were compared on Figs. 12 and 14. The two geogrid types are of different extensibilities (refer to Table II and Fig. 6) and were tested to failure (slippage) under the same values of, σ_{ni} =40 KPa, FL = 1 Hz, and nearly same SPLL = 69 and 58 KN/m for geogrids B and C respectively. It could be noted that the stiffer properties of Geogrid B exhibited higher number of load cycles before slippage. However, the rate of increase in the horizontal displacements with increasing the loading cycles seems to be more affected by the soil properties and not by the geogrid properties. The displacements with load cycles were nearly parallel for both types unlike their performance within the static loading range (Fig. 13). It was also found that the incremental horizontal displacement per cycle decreases with increasing the number of cycles.
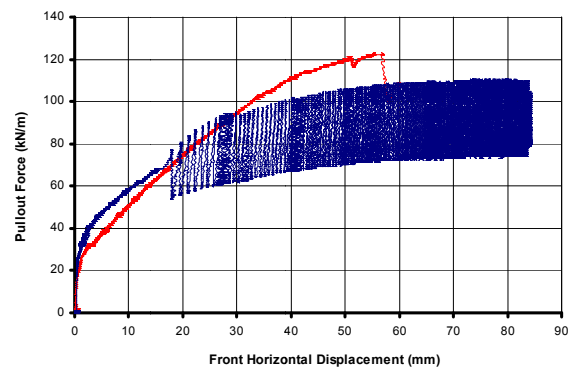

Fig. 10 Static and Cyclic Pullout Tests Results of Geogrid B at (FL=1.0 Hz, σ_{ni} = 37 kPa, SPLL = 70 kPa)
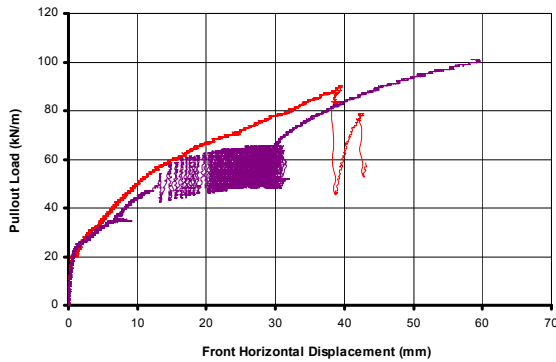
Fig. 11 Static and Cyclic Pullout Tests Results for Geogrid C at
(FL=1.0 Hz, σ_{ni} = 80 kPa, SPLL = 50 kPa)

B. Static Pullout Load Level (SPLL)

Figs. 15 and 16 present cyclic pullout tests results for geogrid (B); performed at the same testing conditions (F_L=0.5 Hz, σ_{ni} = 40 KPa) where the load cycles started at two different Static Pullout Load Levels (SPLL = 45 kN/m and 70 kN/m). The tests were carried out to slippage. The higher initial SPLL reflects a lower safety factor in the anchorage strength of the geogrid in reinforced earth structures. It is clear that the test that started at higher SPLL have reached failure at a lower number of loading cycles. No practical changes in the

rate of the horizontal displacement while increasing the number of load cycles was observed. The same test was performed on geogrid (A) at the same testing conditions (F_L=1.0 Hz, σ_{ni} = 52 & 62 kPa) where the load cycles started at two different static pullout loads (67 kN/m and 80 kN/m). The tests results are shown in Figs. 17 and 18 and the same conclusion could be obtained.
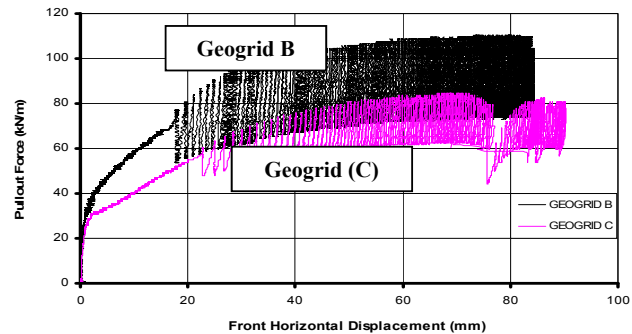

Fig. 12 Comparison of the Pullout Response at Different
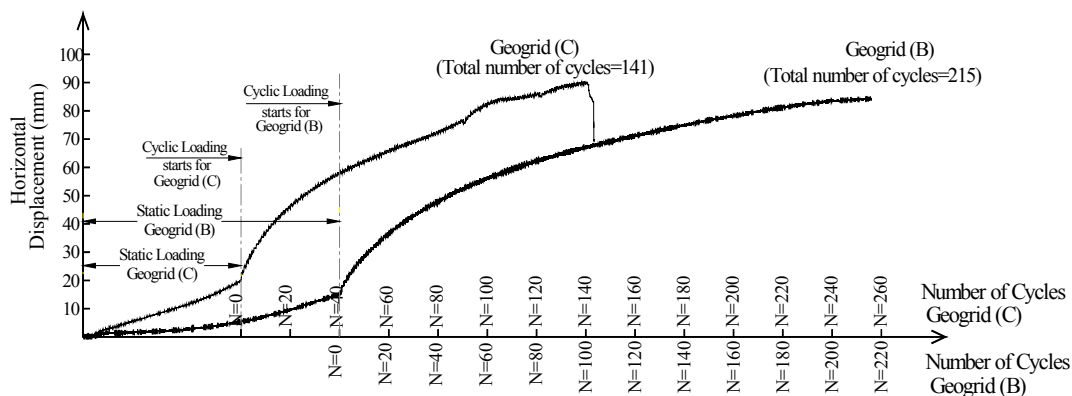Extensibility properties (Geogrids B and C)

Fig. 13 Comparison of Horizontal Displacement Responses during Cyclic Pullout of Different Geogrids Extensibilities (Geogrids B and C)
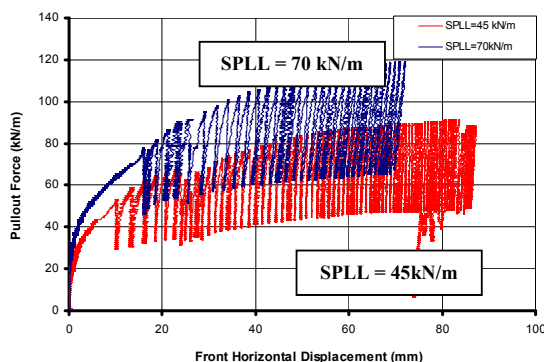

Fig. 14 Comparison of Pullout Responses of Geogrid (B) at Different
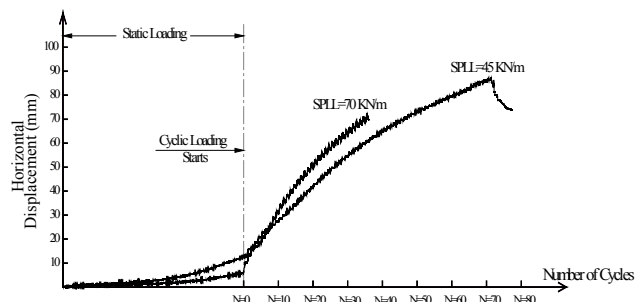Values of SPLL's

Fig. 15 Comparison of Horizontal Displacements along the Geogrid
Sheet with Load Cycles of Geogrid (B) at Different Values of SPLL's

C. Interface Normal Stresses (σ_{ni})

Figs. 19 and 20 present cyclic pullout tests results of geogrid B, performed under similar conditions (F_L=1 Hz, and nearly the same SPLL=78 and 85 kN/m) at two different σ_{ni} (43 kPa and 128 kPa).

The lower σ_{ni} reflects the condition of a relatively shallow sheet of geogrid placed in a reinforced earth wall or similar. The results indicated that the horizontal displacement of geogrids increased at lower σ_{ni}. However, with increasing σ_{ni} and the number of load cycles, the rates of displacement as well as the incremental changes in the relative displacement along the sheets were clearly affected. This should be accounted for in setting the design properties for geogrid sheets at shallow depths in seismically active areas, in order to avoid excessive displacement at the top facing blocks and hence their dis-integration.
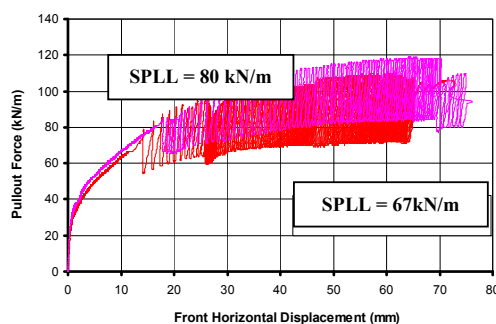

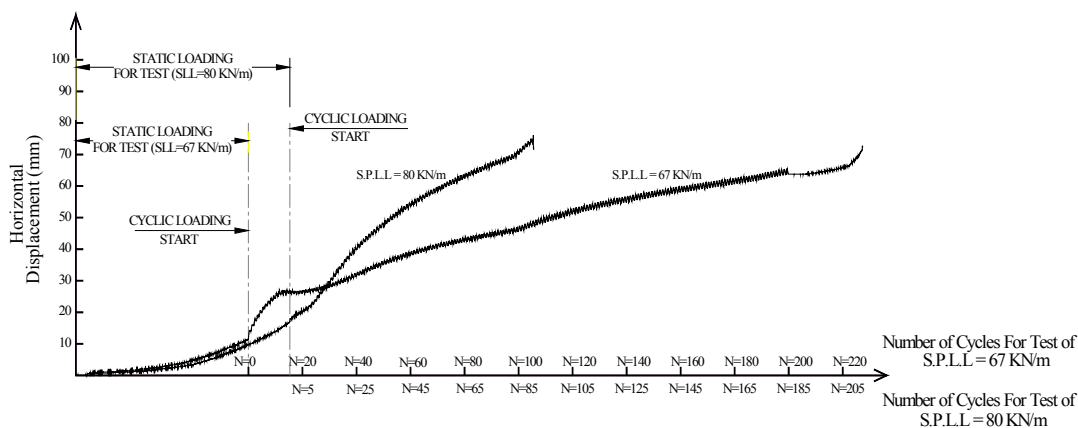Fig. 16 Comparison of Pullout Responses of Geogrid (A) at Different SPLL's

D. Frequency of the Loading Cycles (FL)

Figs. 21 and 22 present the pullout tests results of geogrid C, performed to failure under similar conditions (σ_{ni} = 40 kPa, SPLL= 54 kN/m), and two different loading frequencies (F_L = 0.5 Hz and 1.0 Hz). The displacement per load cycle was found to decrease while increasing load frequency with ability to sustain higher number of load cycles before slippage. However, no effect on the behavior of the displacement with load cycles curves was observed.

E. The Cyclic Loading Amplitude

To investigate the effect of the cyclic loading amplitude on the cyclic pullout response of the embedded geogrids, Fig. 23 presents the tests results of geogrid (C), performed under the same conditions (Normal stress = 80 kN/m², static pullout load = 47 kN/m, and cyclic loading frequency = 1.0 Hz), at two different cyclic loading amplitude, 15 kN/m, and 25 kN/m, which simulates 16%, and 28% of the maximum monotonic pullout resistance. From Fig. 23, the following could be concluded:

1- The displacement per cycle under higher cyclic loading amplitude is higher than displacement per cycle under lower cyclic loading amplitude.

2- For cyclic loading amplitude = 16% of the monotonic pullout resistance, the geogrid could sustain 120 loading cycles. For cyclic loading amplitude = 28% of the monotonic pullout resistance, the geogrid could sustain 74 loading cycles only.

3- The horizontal strain increased from 9.04% to 16.59% for the tests performed at cyclic loading amplitude equal to 16%, and 28% of the monotonic pullout resistance, respectively.
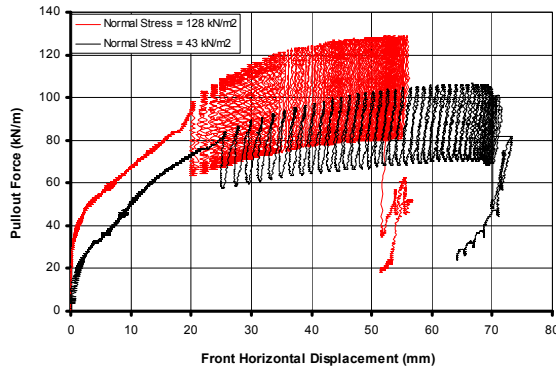

Fig. 17 Comparison of the Horizontal Displacements along the Geogrid Sheet with Load Cycles of Geogrid (A) at Different Values of SPLL's

Fig. 18 Comparison of Pullout Responses of Geogrid (B) at Different Values of σ_{ni}'s
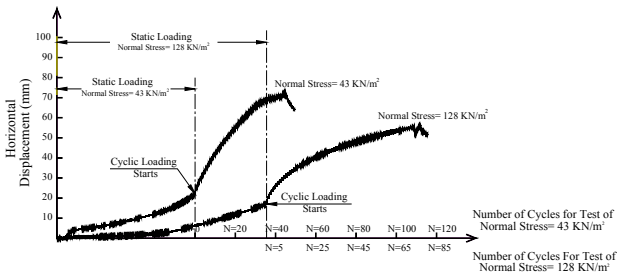

Fig. 19 Comparison of the Horizontal Displacement with Load Cycles of Geogrid (B) at Two Different Values of σ_{ni}'s
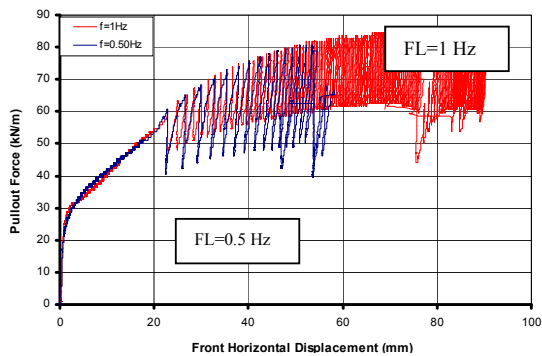

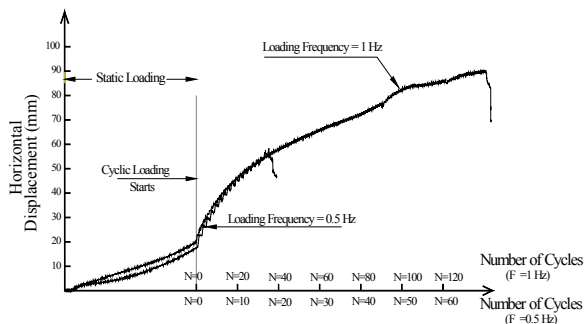Fig. 20 Comparison of Pullout Responses of Geogrid (C) at Different Values of F_L's

Fig. 21 Comparison of Horizontal Displacement with Load Cycles of Geogrid (C) at Two Different Vales of FL's
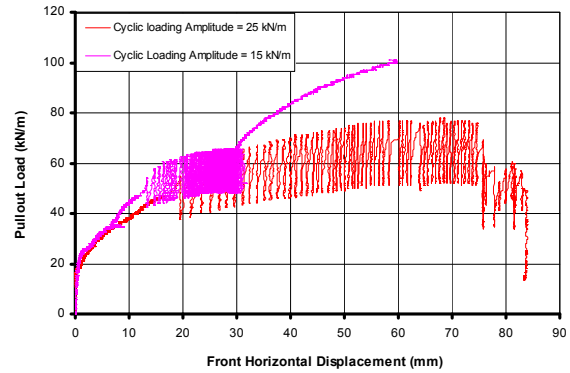

Fig. 22 Comparison of Pullout Responses of Geogrid (C) Subjected to the same Test Conditions at Two Different Cyclic Loading Amplitudes
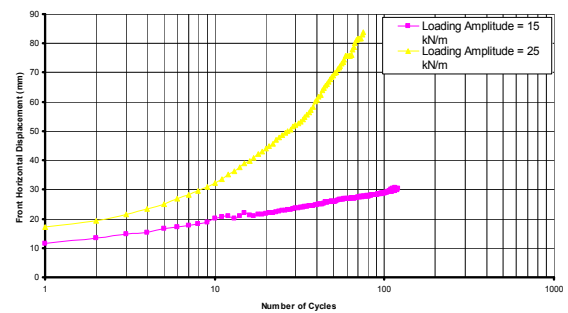

Fig. 23 Comparison of Horizontal Displacement versus Number of Loading Cycles along Geogrid (C) Under the Same Test Conditions at Two Different Cyclic Loading Amplitudes

VIII. DISPLACEMENT MOBILITY OF GEOGRIDS UNDER CYCLIC LOADING

The displacement of the geogrid sheet under cyclic loading could be calculated from (1) as;

$$\Delta_{total} = \Delta_{static} + \Delta_{cyclic} \tag{1}$$

where; Δ_{total}: the total displacement of the geogrid sheet (in monotonic and cyclic loading); Δ_{static} the static displacement at SPLL (could be derived from numerical modeling or from monotonic experimental test) Δ_{cyclic}: the cyclic displacement at number of loading cycles = N, as each loading cycle develop a permanent accumulative displacement in the geogrid.

$$= \Sigma\Delta_{per\ cycle(N=1\ to\ N=N)} = \Delta_{N=1} + \Delta_{N=2} + \Delta_{N=3} + \Delta_{N=4} + \ldots.\Delta_{N=N} \tag{2}$$

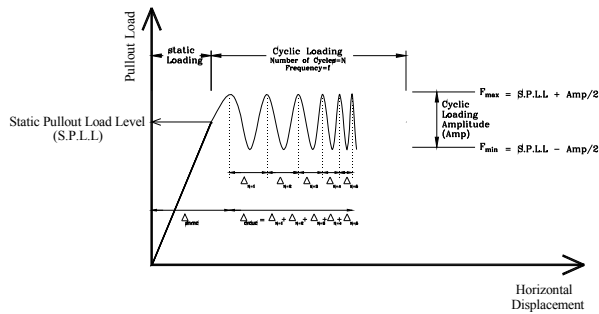Fig. 24 illustrates the notation in (2).

Fig. 24 The Notations Used in Equations 1 and 2

Based on the experimental tests results, conducted during this research, it could be concluded that the horizontal permanent displacement per cycle of the geogrid sheet under cyclic loading depends mainly on the following parameters:

- The number of loading cycles (N),
- The static pullout load level (SPLL),
- The applied normal stresses (σ_n),
- The loading frequency (F_L),
- The cyclic loading amplitude (Amp), and
- The Geogrid sheet stiffness.

The previous parameters should be encountered in the calculation of the displacement of the geogrid sheet under cyclic loading. In this section, the results of the experimental tests were used to develop a relationship between the permanent accumulative displacement per cycle of the geogrid and the number of the loading cycles. The results of twelve cyclic pullout tests were implemented in developing the proposed relationship. The data of these tests are shown in Table III.

The permanent displacements per cycle for the previous twelve tests were plotted with the number of loading cycles, as shown in Fig. 25.

TABLE III
THE TESTS IMPLEMENTED IN DEVELOPING THE PROPOSED RELATIONSHIP FOR THE GEOGRID UNDER THE CYCLIC LOADING

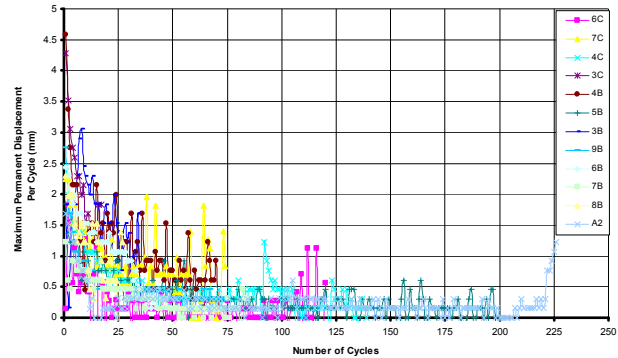| Test number	Geogrid Type	Type of the Test	Initial Normal Stresses (kPa)	SPLL (kN/m)	Load Level (SPLL/P_{ult})	Frequency (Hz)
2A	A	Cyclic	62	67	0.42	1
3B		Cyclic	37.5	70	0.58	0.5
4B		Cyclic	40	45	0.38	0.5
5B		Cyclic	37	70	0.58	1
6B	B	Cyclic	43	75	0.63	1
7B		Cyclic	73	85	0.71	2
8B		Cyclic	70	82	0.68	1
9B		Cyclic	128	90	0.75	1
3C		Cyclic	34	54	0.60	0.5
4C	C	Cyclic	40	54	0.60	1
6C		Cyclic	80	47	0.52	1
7C		Cyclic	80	48	0.53	1

Fig. 25 Maximum Permanent Horizontal Displacement per Cycle versus the Number of Cycles for the Twelve Selected Tests

From Fig. 25 all the curves could be viewed as taking a general trend line for the relationship between the displacement per cycle and the number of loading cycles.

The trend line for all curves could be normalized through the general form in (3):

$$\Delta_{\text{per cycle (N)}} = B - A \times \ln(N) \qquad (3)$$

where; N: Number of loading cycle at which the permanent cyclic displacement is calculated; A, B: Empirical Constants that depend on the applied normal stress, SPLL, cyclic loading amplitude, Cyclic loading frequency, the geogrid sheet extensibility.

Fig. 26 shows the normalized curve for the relationship between the permanent cyclic front horizontal displacement and the number of loading cycles.
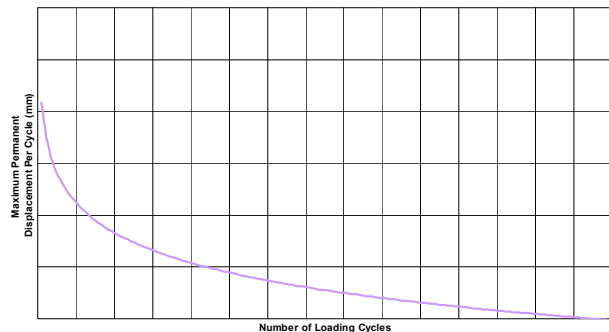

Fig. 26 The Normalized Trend Line for the Relationship between the Permanent Cyclic Front Horizontal Displacement and the Number of Loading Cycles

The values of the constants A, and B are controlled by the SPLL, initial normal stress, geogrid type, cyclic loading amplitude, and frequency. This requires a large number of cyclic pullout tests to be performed with different types of geogrids and cyclic loading conditions to develop an accurate determination for the constants (A, and B).

Empirical values for these constants were calculated based on statistical analyses. It should be noted that these empirical values are limited to the condition of the tests performed during the course of this research (geogrid type, cyclic loading

frequency, the range of normal stresses and the cyclic loading amplitude). The average values were calculated for the constants as;

$$A = 0.33, \text{ and } B = 1.80$$

These empirical constants are limited only to the range of parameters used in this experimental work. Deriving a reliable equation for these constants recommended for further study with wide a range of geogrids types, cyclic loading configurations and initial stress conditions.

IX. SHAPES OF FAILURE OF GEOGRID SHEETS UNDER CYCLIC LOADING

Failure in the geogrid sheet material during cyclic pullout tests was found during the experimental program to occur according to either of the following modes (Fig. 27); (a) Tensile failure in the longitudinal ribs, b) Junction failure, (c) flexural or shear failure in the transverse ribs. The failure mode was primarily dependent on the stiffness of the geogrid sheet.

Mode of Sample Failure	Shape of the Failure
a) Tensile failure in the longitudinal ribs	
b) Junction failure	
c) Combination of the Tensile Failure in Longitudinal Ribs and Junction Failure (for Softer Geogrids)	

Fig. 27 Modes of Failures of the Geogrids during the Experimental Program

X. CONCLUSIONS

1. The horizontal displacements and the horizontal strain of the geogrid sheets are higher in case of cyclic loading than monotonic loading due to cyclic mobility.
2. The distribution of horizontal displacement under the cyclic loading is more flat than distribution under monotonic loading.
3. The horizontal displacements of geogrids under cyclic loading increases with increasing the number of load cycles till full slippage.
4. The geogrid sheets of relatively low tensile strength are not recommended for the reinforced earth structures that are subjected to cyclic loading, even if they can statically be proven safe.
5. The static pullout load (SPLL) at which the cyclic loading starts affect the performance of the geogrid sheet under the cyclic loading. The displacement of the geogrid sheet increase with increasing the static pullout load at which cyclic loading starts. In addition, the number of loading cycles, which the geogrid sheet can sustain, decreases with increasing the static load at which the cyclic loading starts.
6. Higher static safety factors against geogrid slippage results in a more resilient performance during cyclic loading and accordingly earthquakes.
7. Incremental horizontal displacement per load cycle of geogrids increase at lower interface normal stresses. This should be accounted for in setting the design parameters for geogrid sheets placed at shallow depths in seismically active areas. This will also lead to avoiding excessive displacements near the facing top levels which might result in partial disintegration to the facing blocks.
8. The displacement per load cycle increase with decreasing the load frequency.
9. The displacement per cycle, total displacement, and strain under higher cyclic loading amplitude is higher than case of lower cyclic loading amplitude.
10. The number of cycles that geogrid could sustain, for case of high cyclic loading amplitude, is lower than the number of loading cycles for low cyclic loading amplitude.
11. The permanent displacement per cycle depends on the geogrid extensibility, number of loading cycles, applied normal stress, static pullout load level, cyclic loading amplitude, and loading frequency.
12. The horizontal displacements of the initial loading cycles are higher than the horizontal displacement at the subsequent loading cycles. In other words, the horizontal displacements per cycles decrease with increasing the number of loading cycles.
13. The failure in the geogrid sheet in cyclic pullout tests may occur according to one of the following modes; (a) Tensile failure in the longitudinal ribs, (b) flexural or shear failure in the transverse ribs, and (c) Junction failure.

REFERENCES

[1] Abdel-Rahman, A., Ashmawy, A.K., Abdel-Moniem, M., "An Apparatus for Direct Shear, Pullout and Uniaxial Testing of Geogrids" *Geotechnical Testing Journal, ASTM, Vol. 1, No.4, 2007, pp.415-430.*
[2] Bathurst, R.J., and Cai, Z., "Pseudo-Static Seismic Analysis of Geosynthetic Reinforced Segmental Retaining Walls", *Geosynthetic International, Vol.2, No.5, 1995, pp. 787-830.*
[3] Fannin, R. and Raju, D, "Large-Scale Pullout Test Results on Geosynthetics", Vancouver, Canada-Geosynthetics, 1993.

[4] Ling, H.I., DovLeshchinsky, Jui-Pin Wang, Yoshiyuki Mohri, and Arik Rosen, "Seismic Response of Geocell Retaining Walls", Experimental Studies",*Journal of Geotechnical and Geo-environmental Engineering, ASCE / APRIL 2009, pp.515-52*.

[5] Ling, H.I., Leshchinsky, D., and ChouN.S., "Post-Earthquake Investigation on Several Geosynthetic-Reinforced Soil Retaining Walls and Slopes during the Ji-Ji Earthquake of Taiwan", *Soil Dynamics and Earthquake Engineering, Vol 21, 2001, pp. 297-313.*

[6] Nayeri, A., and Fakharian, K., "Study on Pullout Behavior of Uniaxial HDPE GeogridsUnder Monotonic and Cyclic Loads*", International Journal of Civil Engineering, Vol.7, No.4, Dec 2008.*

[7] Pacific earthquake Engineering research center (PEER), Some Observations of Geotechnical Aspects of the February 28, 2001, Nisqually Earthquake in Olympia, South Seattle, and Tacoma, Washington.

[8] Pamuk, A., Hoe I. Ling, DovLeshchinsky, ErolKalkan, KorhanAdalier, "Behavior of Reinforced Wall System During the 1999 Kocaeli (IZMIT), Turkey Earthquake.", *Fifth international conference on case Histories in Geotechnical Engineering, New York, April 2004.*

[9] Palmeira, M. E., "Bearing force mobilisation in pull-out tests on geogrids", *Geotextiles and Geomembranes, Vol. 22, pp.481-509, 2004.*

[10] Sankey, J.E., and Segrestin, P., "Evaluation of Seismic Performance in Mechanically Stabilized Earth Structures", The Reinforced Earth Company, Vienna, Virginia, USA 2001.

[11] Wartman, J., Efrain A. Rondinel, and Adrian Rodriguez-Marek., "Performance and Analyses of Mechanically Stabilized Earth Walls in the Tecomán, Mexico Earthquake", *Journal of Performance of Constructed Facilities, Vol. 20, No. 3, August 1, 2006.*

[12] Wilson-Fahmy, R.F., Koerner, R.M., and Sansone, L.J., "Experimental Behavior of Polymeric Geogrids in Pullout", *Journal of Geotechnical Engineering, Vol. 120, No. 4, Apr., 1994.*